Surface-morphology evolution during unstable homoepitaxial growth of GaAs(110)

P. Tejedor*
Semiconductor Materials IRC, Imperial College, London SW7 2BZ, United Kingdom and Instituto de Ciencia de Materiales de Madrid (C.S.I.C.), Cantoblanco, 28049 Madrid, Spain

P. Šmilauer
Institute of Physics, Academy of Sciences of the Czech Republic, Cukrovarnická 10, 162 53 Praha 6, Czech Republic and Semiconductor Materials IRC, Imperial College, London SW7 2BZ, United Kingdom

C. Roberts and B. A. Joyce
Semiconductor Materials IRC, Imperial College, London SW7 2BZ, United Kingdom
(Received 16 April 1998)

The time evolution of the surface morphology during growth of GaAs(110) by molecular-beam epitaxy is studied using Nomarski and atomic force microscopy. Depending on the growth temperature and As_4 overpressure, different types of growth instabilities are observed: large three-dimensional pyramidal features develop under As-deficient growth conditions, whereas step bunching takes place under As-rich conditions. In addition, a crossover from step bunching, attributed to a negative step-edge barrier, to unstable growth typical of a positive step-edge barrier, takes place under As-deficient conditions as the film thickness increases. Under suitable growth conditions, self-organization of the microscopic features during growth leads to the creation of a highly unusual, well-ordered pattern on the surface. We discuss the microscopic origin of the observed instabilities with the help of recent theoretical and experimental results. [S0163-1829(99)05803-8]

Instabilities and facet formation during epitaxial growth have been traditionally perceived as an obstacle standing in the way of preparing smooth surfaces. However, a recent research trend exists that tries to *use* three-dimensional (3D) surface features created by such instabilities to fabricate laterally ordered nanostructures. For successful applications, it is imperative to achieve a regular spatial arrangement and narrow size distribution of these features, which requires a thorough understanding of the details of the growth process.

A great deal of attention has recently been focused on unstable growth caused by the so-called Ehrlich-Schwoebel (ES) effect,[1,2] i.e., by additional barriers to adatom hopping at step edges. Due to these barriers that hinder interlayer transport, 3D features (pyramids or mounds) appear during growth on a high-symmetry (singular) surface, forming a pattern with a characteristic lateral dimension that usually increases with the film thickness.[3] Much less attention has been paid to instabilities that occur during growth of miscut (vicinal) surfaces consisting of flat terraces separated by steps.

In a classical paper, Schwoebel and Shipsey[2] analyzed a simple 1D model of growth in the so-called step-flow mode on a vicinal surface, where growth proceeds mainly by incorporation of adsorbed atoms into edges of pre-existing steps. These authors demonstrated that the ES effect tends to equalize terrace sizes because, when adatoms cannot easily leave the terrace on which they were deposited (due to the additional energetic barrier for downward hops), the ascending steps adjacent to large terraces advance faster than those adjacent to small terraces. However, Schwoebel and Shipsey neither explored the time evolution of the step train in detail nor dealt with the physically relevant case of a 2D surface. The latter problem was addressed by Bales and Zangwill[4] (BZ), who pointed out that during step-flow growth in the presence of the ES barriers on a vicinal 2D surface, the steps themselves can become unstable due to a preferential attachment of adatoms to advanced parts of the steps. These authors did not, however, study the long-time evolution of the surface.

Very recently, Rost, Šmilauer, and Krug[5] investigated step-flow growth in the presence of the ES barriers, using numerical integration of an equation of motion and kinetic Monte Carlo (KMC) simulations to explore the nonlinear, late-stage regime. They observed the BZ instability with steps meandering in phase, creating surface ripples along the direction of the tilt [Fig. 1(a)]. As growth proceeds, a secondary instability sets in, and ripples break up into pyramid like mounds similar to those observed during growth on a high-symmetry surface,[5] cf. Fig. 1(b).

Schwoebel and Shipsey[2] also analyzed the opposite case, in which adatoms attach to steps more easily from the upper terrace, and found that this makes the 1D step train unstable against fluctuations in terrace sizes leading eventually to formation of step bunches. This mechanism was invoked by Krishnamurthy *et al.*[6] to explain quasiperiodic faceting during homoepitaxy on GaAs(110) vicinal surfaces.[6,7]

In this paper, we examine the temporal evolution of the surface morphology during homoepitaxial growth by molecular-beam epitaxy (MBE) on GaAs(110) vicinal substrates at different temperatures and V:III flux ratios. In addition to step bunching, we find a variety of other pattern-forming instabilities depending both on the growth conditions used and on the thickness (time evolution) of the growing layer.

The experiments were carried out in a standard VG V80H MBE system equipped with a 15-keV electron gun for reflec-

0163-1829/99/59(3)/2341(5)/$15.00 PRB 59 ©1999 The American Physical Society

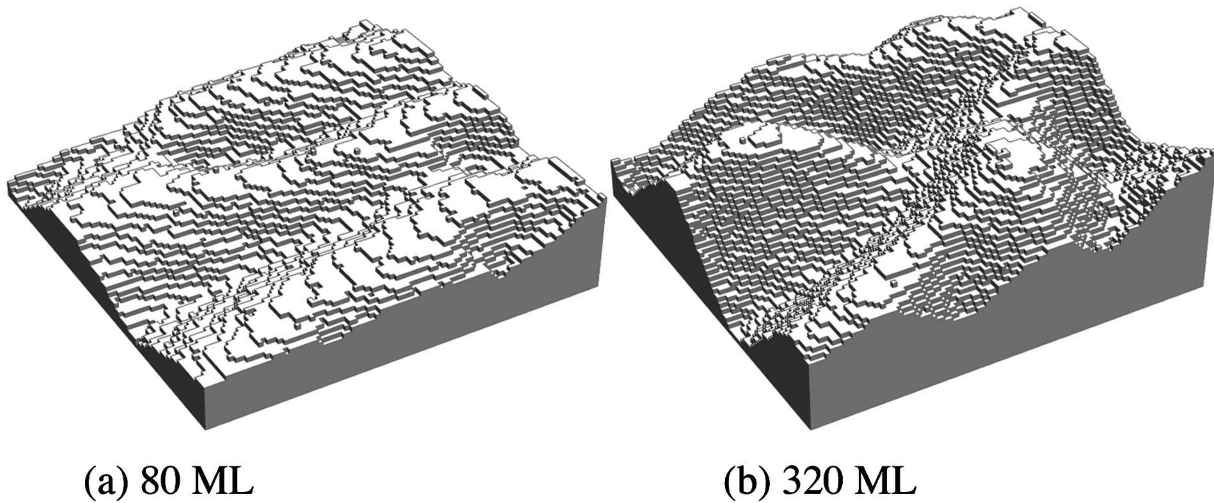

FIG. 1. Surface morphology in KMC simulations with an additional hopping barrier at the step edges. The monolayer steps become wavy due to the Bales-Zangwill instability (Ref. 4), and self-organize, creating ripples running in the direction of the tilt (a). Subsequently, the ripples break down starting at the defects of the ripple pattern, and 3D features appear on the surface (b).

tion high-energy electron-diffraction (RHEED) measurements. Arsenic was supplied using a standard As_4 source. The growth temperature was measured using an Ircon pyrometer referenced to the transition temperature of surface reconstruction from GaAs(001)-$c(4\times4)$ to 2×4 (520 °C under an As_4 flux equivalent to $2\,\mathrm{ML\,s^{-1}}$). Ga and As_4 fluxes were calibrated using RHEED intensity oscillations on a GaAs(001) substrate. The epiready semi-insulating GaAs(110) substrates misoriented towards (111)A by 1.5° (American Xtal Technology) were indium bonded to molybdenum disks and outgassed in vacuum at 300 °C overnight. The substrates were then transferred to the growth chamber, where the native oxide layer was removed at 610–620 °C under an As_4 flux of 4×10^{16} molecules $\mathrm{cm^{-2}\,s^{-1}}$. Subsequently, GaAs layers whose thicknesses ranged from 2 to 3000 Å were grown at 500–550 °C. The Ga flux was 6×10^{13} atoms $\mathrm{cm^{-2}\,s^{-1}}$ in all experiments, while the As_4 flux was adjusted to provide different As:Ga flux ratios. Under these conditions, the GaAs growth rate on the (110) surface was 0.14 $\mathrm{ML\,s^{-1}}$. Three sets of samples were grown, hereafter referred to as *A*, *B*, and *C*. Set *A* (film thicknesses: 25, 100, 250, and 1500 ML) was grown at 500 °C with an As:Ga flux ratio of 23:1. Set *B* (film thicknesses: 1, 10, 100, 250, and 500 ML) was grown at 550 °C with an As:Ga flux ratio of 7:1. Set *C* (film thicknesses: 25, 100, 250, and 1500 ML) was grown at 500 °C with an As:Ga flux ratio of 7:1. Immediately after growth, all samples were quenched to room temperature, with the arsenic cell shutter open down to 400 °C to avoid any modification of the as-grown surface morphology by annealing.

The surface morphology of the epitaxial layers was examined by optical Nomarski microscopy and atomic force microscopy (AFM) using a commercial instrument (AFM PSPM Burleigh Instruments, Inc.) working in the constant force contact mode at a scan rate of 0.35 lines per second and 256 points per line scan. Etched single-crystal silicon tips were used with an end radius of 100 Å and a sidewall angle of 35.3°.

The samples from series *A*, which were grown at 500 °C with an As:Ga flux ratio of 23:1, exhibit the formation of macrosteps by step bunching studied in previous papers on GaAs(110) homoepitaxy.[6,7] Figures 2(a)–2(c) are 4×4-$\mu\mathrm{m}^2$ AFM images showing the surface morphology evolution and their corresponding cross sections, all taken along the [001] direction, after deposition of 25, 100, and 1500 ML of GaAs, respectively. The effect of saturation of the average distance between macrosteps discussed in Ref. 6 is also observed in our case, the average terrace width at saturation being around ≈4000 Å, with the average macrostep height of ≈120 Å. One can even detect a certain degree of self-organization of macrostep undulations [Fig. 2(c)], although it is weak due to the large distances between them.

A considerably lower As_4 overpressure (As:Ga=7:1) was used to grow the samples in series *B* and *C* and, consequently, their surface morphology undergoes a very different time evolution. The 5×5-$\mu\mathrm{m}^2$ AFM images shown in Figs. 3(a)–3(c) illustrate the surface morphology evolution in series *B*, after deposition of 10, 100, and 500 ML, respectively, at 550 °C. Initially [Fig. 3(a)], limited step bunching leads to creation of 4–10-Å high steps [the (110) interplanar distance is 1.999 Å]. Thereafter, the steps become wavy and partially self-organize, forming interwoven ridges running parallel to the surface tilt, as shown in Fig. 3(b). Eventually, large 3D triangular features appear on the surface [Fig. 3(d)], superimposed onto the cellular background shown in Fig. 3(c). This evolution closely follows the results obtained in Ref. 5 where it was demonstrated how a secondary instability leads to the creation of 3D pyramidal features at defects of the ripple pattern; cf. Fig. 1. Our results thus appear to be an experimental confirmation of the theoretical predictions of Ref. 5.

A similar morphological evolution takes place for set *C* grown at 500 °C, but it is much more dramatic and unexpected, as can be seen in the AFM images (4×4 $\mu\mathrm{m}^2$) shown in Figs. 4(a)–4(c). Initially, step bunching takes place creating a disordered structure [Fig. 4(a)] with macrosteps several tens of monolayers high. Subsequently, the steps develop triangular ''teeth'' [Fig. 4(b)] (cf. also Ref. 8), whose shape has its origin in both energetics and kinetics of step formation on a GaAs(110) surface.[9] The cross-section profile of the teeth (not shown) strongly resembles the 3D features

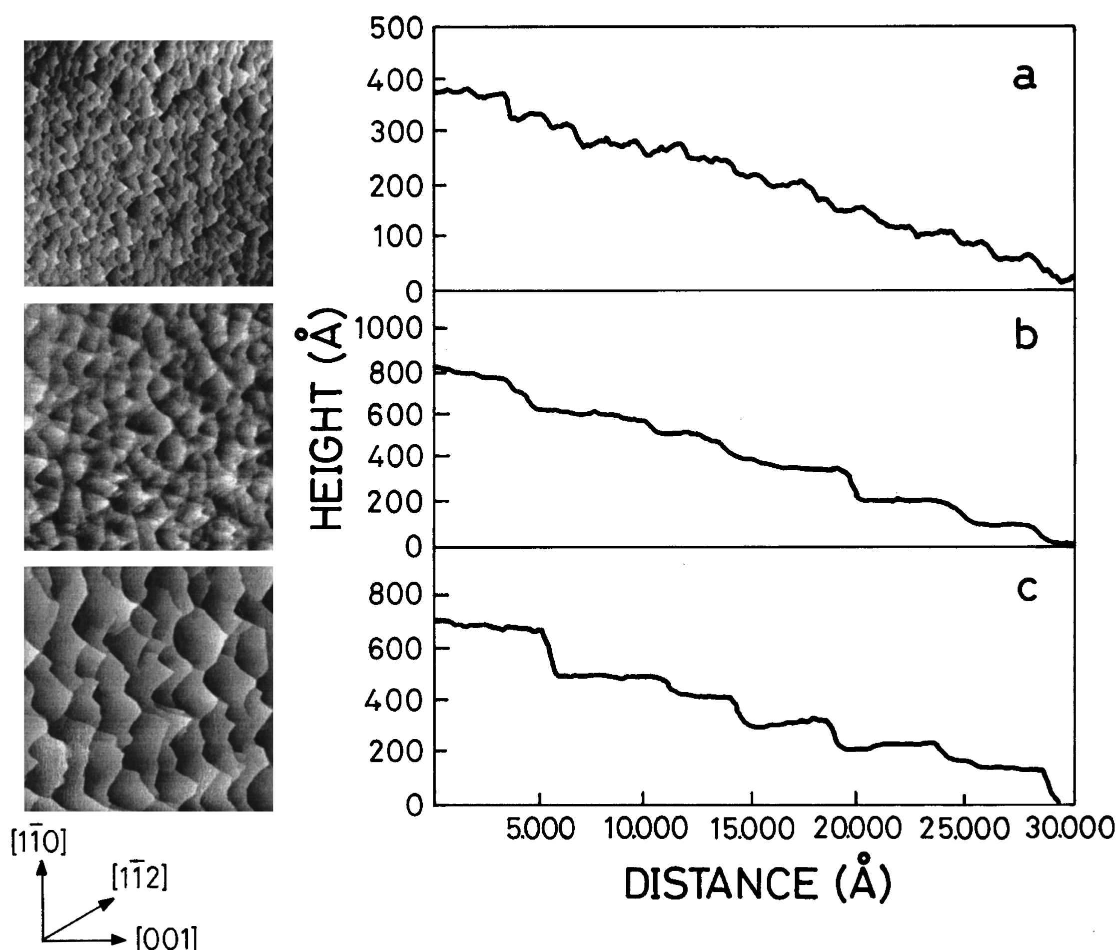

FIG. 2. AFM images (4×4 μm^2) and their corresponding cross sections along the [001] direction, showing the evolution of the GaAs(110) vicinal surface morphology upon deposition of (a) 25 ML, (b) 100 ML, and (c) 1500 ML of GaAs at a substrate temperature of 500 °C and an As/Ga flux ratio of 23.

created during epitaxy on the GaAs(110) singular surface.[10] These triangular features subsequently coarsen and self-organize [Fig. 4(c)], due to their interaction mediated by diffusing adatoms. This self-organization, shown in cross section along the [001] direction in Fig. 5, is similar to in-phase ordering of wavy steps generated by the simulation in Ref. 5 [cf. Fig. 1(a)], albeit on a very different length scale. The resulting surface morphology, observed by Nomarski microscopy (Fig. 6) and AFM [Fig. 4(c)], is a particularly interesting example of a laterally ordered surface pattern. Our results thus suggest a possibility of controlled patterning of surfaces by fine tuning the growth conditions.

The results described above can be understood with the aid of the kinetic analysis of GaAs homoepitaxial growth using As_4 on the (110) singular surface performed by Tok *et al.*[11] Extrapolation of their data indicates that when one grows under a Ga flux as low as the one used in our experiments (6×10^{13} atoms cm^{-2} s^{-1}), and As is supplied in excess, the GaAs growth rate is determined by the rate at which the incident Ga atoms are incorporated at step edges. This is clearly the case for the samples of series *A*, grown at 500 °C and at an As:Ga flux ratio of 23:1. The fact that step bunching is observed in this series regardless of sample thickness thus implies that the incorporation of Ga adatoms at step edges from the upper terrace is the rate-limiting step,[12] and results in a ''negative'' ES effect. The same mechanism is responsible for the step-bunching instability observed initially in the samples of series *C*, although they were grown at a much lower flux ratio, but at the same comparatively low temperature. Such a negative ES barrier can be explained on the atomistic level by the high activation energy for incorporation of diffusing Ga adatoms into the experimentally observed [$1\bar{1}2$]-type step edges when coming from the lower terrace. According to recent theoretical calculations by McCoy and LaFemina,[9] the reason for such a high activation energy is that the charge density of dangling bonds of [$1\bar{1}2$] step-edge atoms can rehybridize by the creation of vacancies along the step line, possibly accompanied by step-edge rebonding via formation of dimers, resulting in very stable autocompensated steps.

A significantly different evolution of the surface morphology is observed in the samples of series *B* and *C*, grown at an As:Ga flux ratio of 7:1. The difference can be attributed to a much lower arsenic population available for reaction in comparison with the samples in series *A*. The effective arsenic population in series *B*, grown at 550 °C, is considerably lower than for series *C*, because the incorporation coefficient of As_4 on the GaAs(110) surface decreases with growth temperature from 0.15 at 500 °C to 0.10 at 550 °C.[11] As a result, the population of atomic As on the surface for series *B* is almost equal to the incident Ga flux, and growth takes place

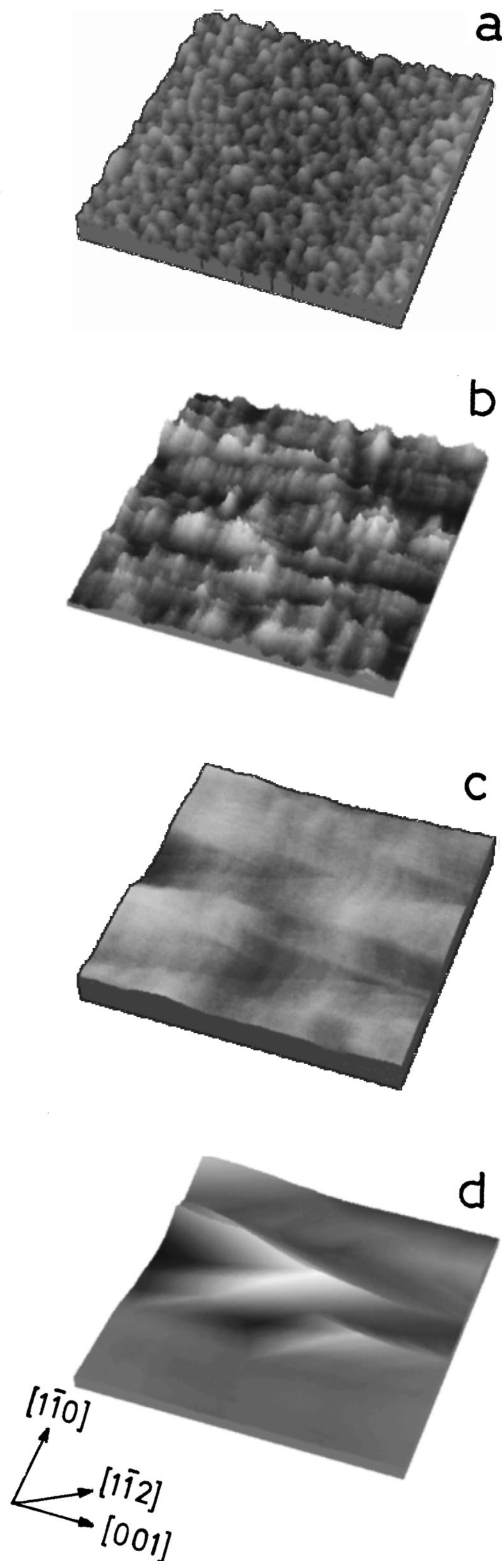

FIG. 3. AFM images (5×5 μm^2) of the GaAs(110) vicinal surface after deposition of (a) 10 ML, (b) 100 ML, (c) 500 ML (cellular background), and (d) 500 ML (3D pyramidal mounds) of GaAs at a substrate temperature of 550 °C and an As/Ga flux ratio of 7.

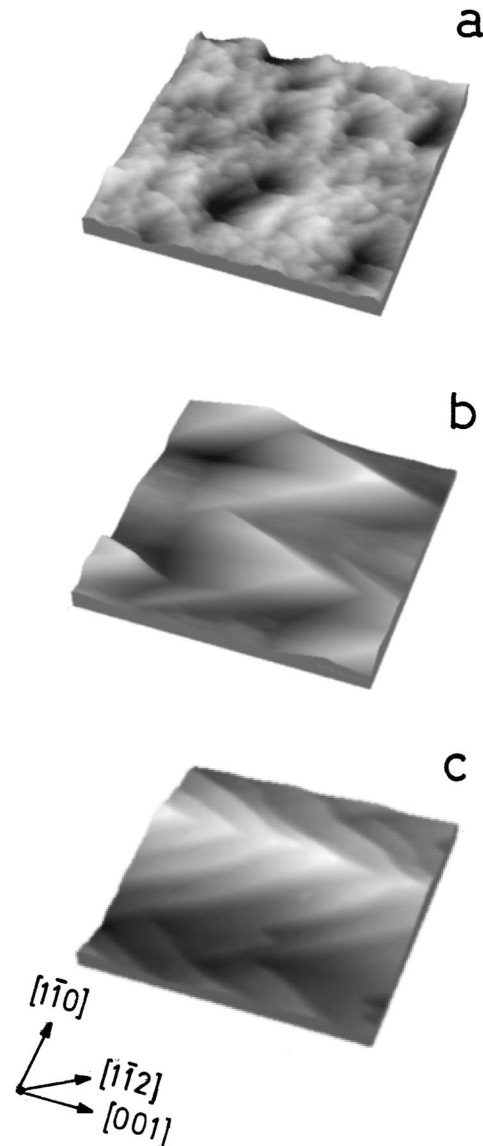

FIG. 4. AFM images (4×4 μm^2) showing the evolution of the GaAs(110) vicinal surface morphology upon deposition of (a) 25 ML, (b) 100 ML, and (c) 1500 ML of GaAs at a substrate temperature of 500 °C and an As/Ga flux ratio of 7.

in conditions close to the As-limited growth regime. Therefore, the incorporation of atomic As into the steps occurring via dissociation of a molecularly adsorbed $As_2^\star$ intermediate[11] plays a decisive role. Since this process occurs preferentially from the lower terrace,[12] a positive ES barrier is observed.

The most dramatic evolution is, however, observed in series *C*. At first, incorporation of Ga adatoms into steps from the lower terraces is hindered, and step bunching takes place similar to series *A*. However, the situation radically changes after a certain thickness is reached. The observed surface morphology evolution at long times closely resembles the predictions of Ref. 5, and suggests that the macrosteps possess a positive ES barrier. This unprecedented *reversal of the sign* of the ES barrier *during growth* indicates a change in step attachment kinetics and disappearance of a ''negative'' ES effect for macrosteps of a certain height.

Our microscopic explanation of this striking phenomenon is based on the fact that [001] type ''nanofacets'' are created on step bunches, as discussed in Ref. 10. Such ''nanofacets'' can [as known from numerous studies of growth on

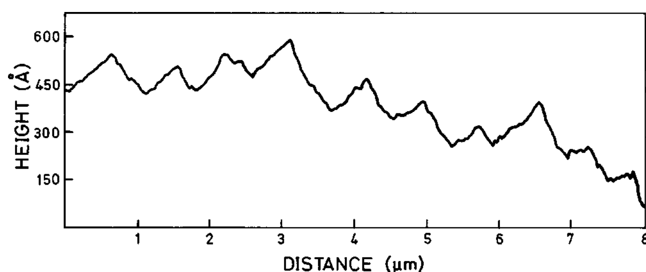

FIG. 5. AFM cross-section scan along the [001] direction for the sample shown in Fig. 4(c), illustrating the self-organization of the 3D features depicted in Fig. 4(b).

GaAs(001) surfaces] readily accommodate Ga adatoms incoming from the lower terraces. The As incorporation thus again becomes the rate-limiting step, and behavior corresponding to a positive step-edge barrier is observed similar to series *B*.

In conclusion, we have experimentally studied homoepitaxial growth on the GaAs(110) surface, and found different pattern-forming instabilities, including previously investigated step bunching attributed to a ''negative'' ES effect as well as unstable growth evolution that can be understood as a result of a ''positive'' ES effect. The surface morphology evolution is found to depend in a crucial way on the availability of As on the surface. In particular, a very unusual phenomenon is observed when initial step bunching in the Ga supply-limited regime is followed by creation of surface ripples and 3D features, implying opposite signs of the ES barrier for isolated steps and macrosteps created by step bunching. We explain this reversal of the sign of the step-edge barrier during growth as a result of different Ga incorporation probabilities on the (110) vicinal surface and on the (001) oriented ''nanofacets'' created on step bunches. The observed self-organization of the 3D features on the surface suggest the possibility of preparing laterally well-ordered arrays of nanostructures by careful adjustment of the growth conditions.

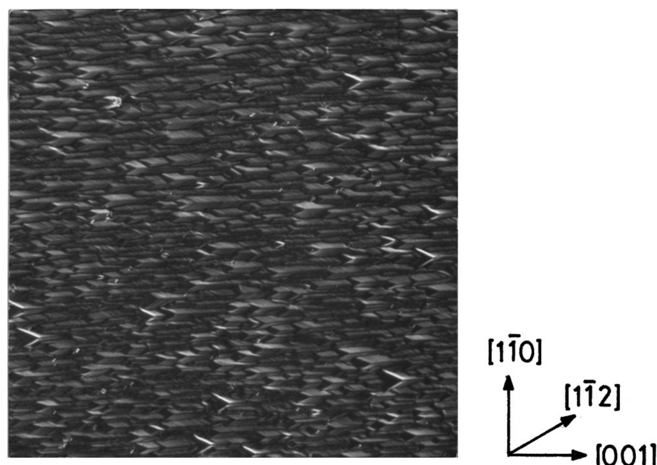

FIG. 6. Nomarski microscopy image (150×150 μm^2) of the self-organized GaAs vicinal surface after the deposition of 1500 ML of GaAs at a substrate temperature of 500 °C and an As/Ga flux ratio of 7, cf. also Fig. 4(c).

This work was supported by the Engineering and Physical Sciences Research Council (EPSRC), UK, under Grant No. GR/97540. P.T. gratefully acknowledges helpful discussions with J.H. Neave and financial support from Ministerio de Investigación y Ciencia of Spain. P.Š. acknowledges fruitful discussions with J. Krug, and financial support from the Alexander von Humboldt Foundation, the Volkswagen Stiftung, the Royal Society, and Grant No. 202/96/1736 of the Grant Agency of the Czech Republic.

*Author to whom correspondence should be addressed. FAX: (+34 1) 3720623. Electronic address: ptejedor@panidi.icmm.csic.es

[1] G. Ehrlich and F. G. Hudda, J. Chem. Phys. **44**, 1039 (1966).
[2] R. L. Schwoebel and E. J. Shipsey, J. Appl. Phys. **37**, 3682 (1966).
[3] J. Krug, Adv. Phys. **46**, 139 (1997).
[4] G. S. Bales and A. Zangwill, Phys. Rev. B **41**, 5500 (1990).
[5] M. Rost, P. Šmilauer, and J. Krug, Surf. Sci. **369**, 393 (1996).
[6] M. Krishnamurthy, M. Wassermeier, D. R. M. Williams, and P. M. Petroff, Appl. Phys. Lett. **62**, 1922 (1993).
[7] S. Hasegawa, M. Sato, K. Maehashi, H. Asahi, and H. Nakashima, J. Cryst. Growth **111**, 371 (1991); R. Nötzel, L. Däweritz, N. N. Ledentsov, and K. Ploog, Appl. Phys. Lett. **60**, 1615 (1992).
[8] D. M. Holmes, E. S. Tok, J. L. Sudijono, T. S. Jones, and B. A. Joyce, J. Cryst. Growth **192**, 33 (1998).
[9] J. M. McCoy and J. P. LaFemina, Phys. Rev. B **54**, 14 511 (1996).
[10] D. M. Holmes, J. G. Belk, J. L. Sudijono, J. H. Neave, T. S. Jones, and B. A. Joyce, Surf. Sci. **341**, 133 (1995).
[11] E. S. Tok, J. H. Neave, F. E. Allegretti, J. Zhang, T. S. Jones, and B. A. Joyce, Surf. Sci. **371**, 277 (1997).
[12] P. Tejedor, F. E. Allegretti, P. Šmilauer, and B. A. Joyce, Surf. Sci. **407**, 82 (1998).